

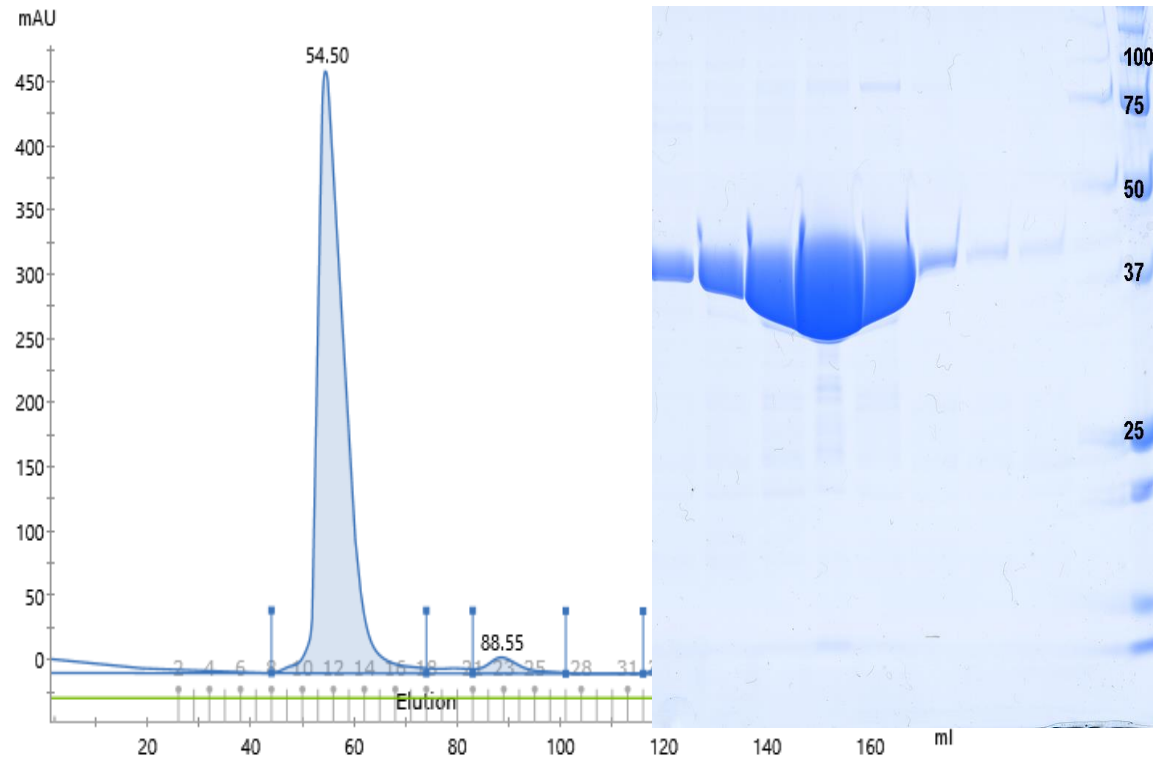
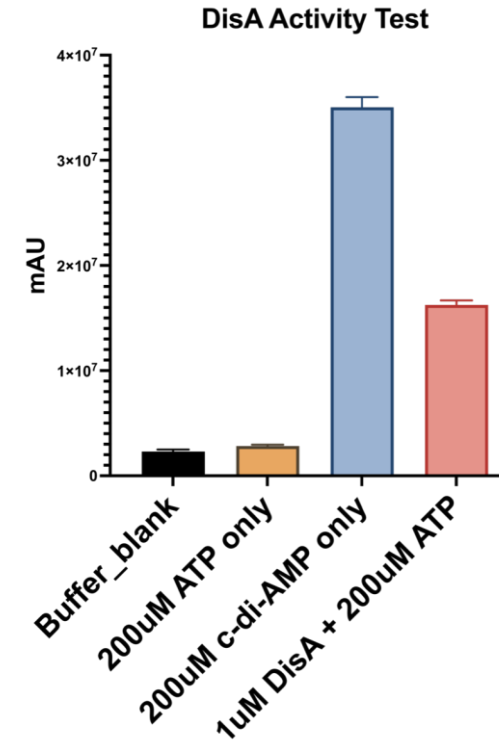
A**B**

Figure 1: Purification of Mtb DisA and its activity assay. A: Size exclusion chromatography profile of Mtb DisA (left) along with the SDS-PAGE of the peak fractions (right). **B:** Results from the fluorescence-based assay that specifically detects c-di-AMP.

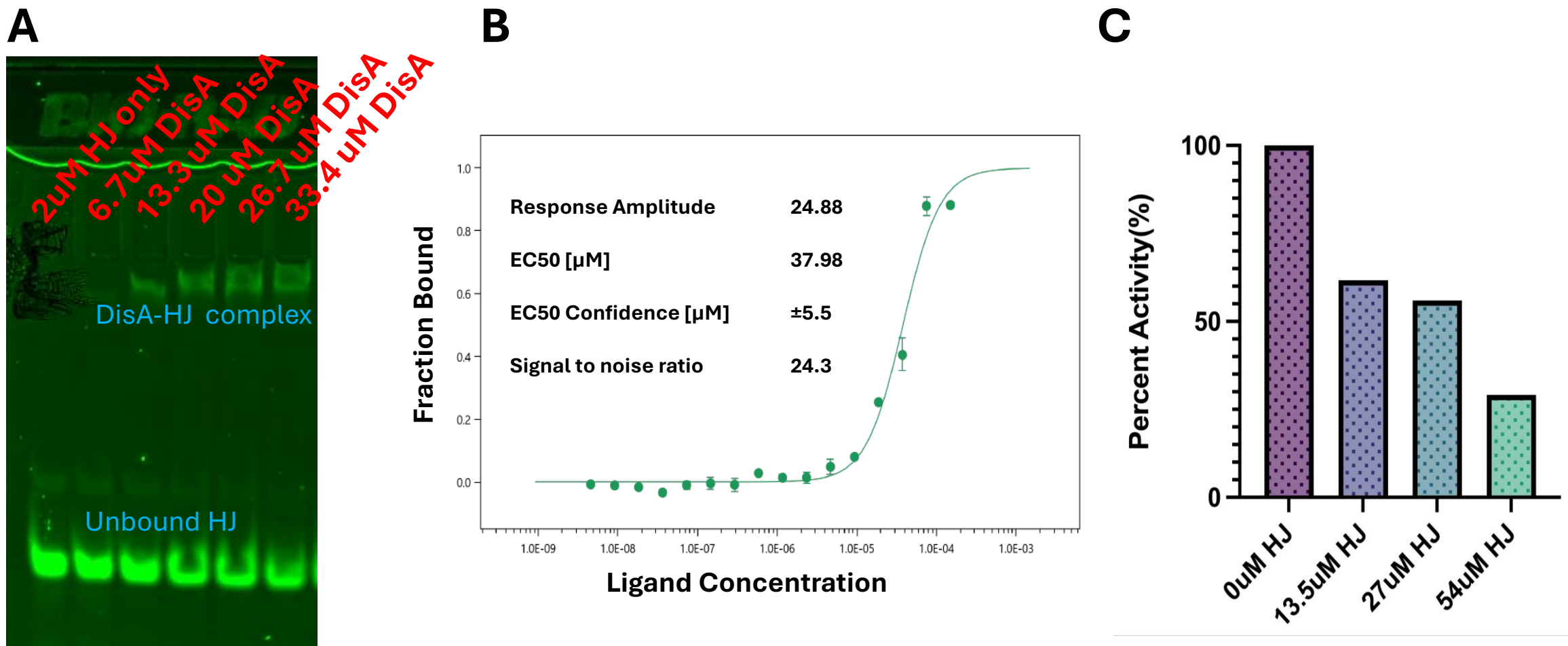
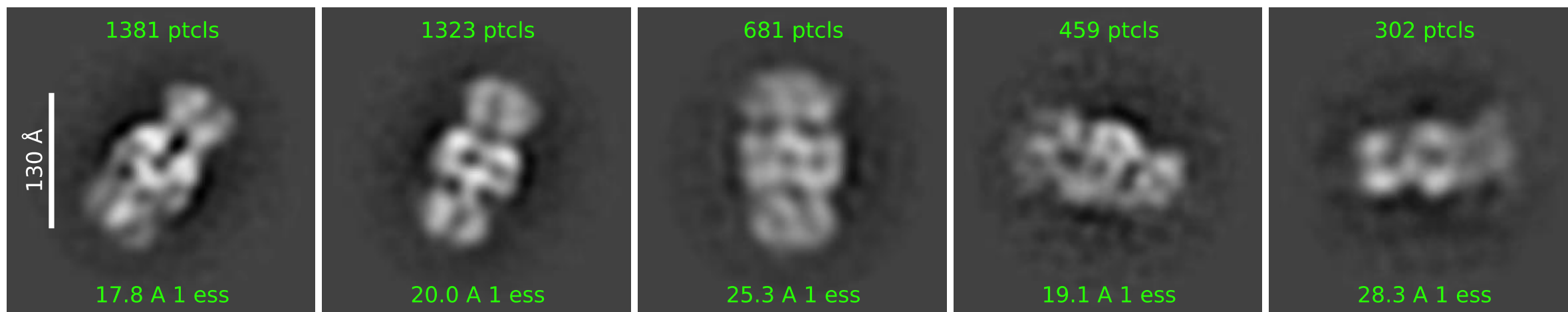


Figure 2: DisA-HJ binding and inhibition of DisA's catalytic activity. A: Electrophoretic mobility shift assay of DisA against HJ. HJ concentration is kept at 2 μ M at all lanes whereas DisA concentration is increased. **B:** Microscale thermophoresis binding curve of DisA-HJ interaction. **C:** Relative activity of DisA (10 μ M) in the presence of increasing concentrations of HJ.

0.5uM DisA



0.5uM DisA + 20uM HJ

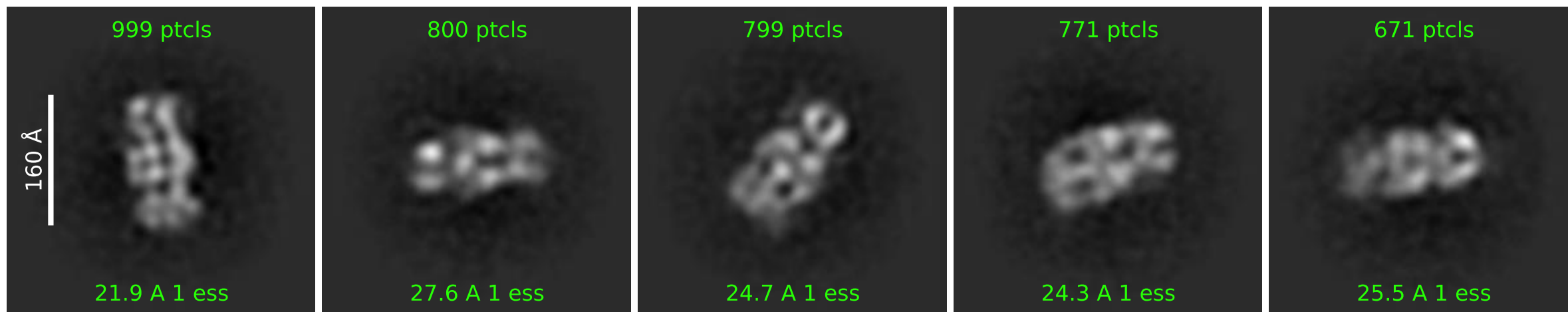


Figure 3: 2D class averages of DisA and DisA-HJ from negative staining. Top: 0.5 μ M DisA alone stained with 2% uranyl acetate. **Bottom:** 0.5 μ M DisA in the presence of 20 μ M HJ stained with 2% uranyl acetate. Class averages were generated using Cryosparc package. (not that the scale bars are different in two graphs).

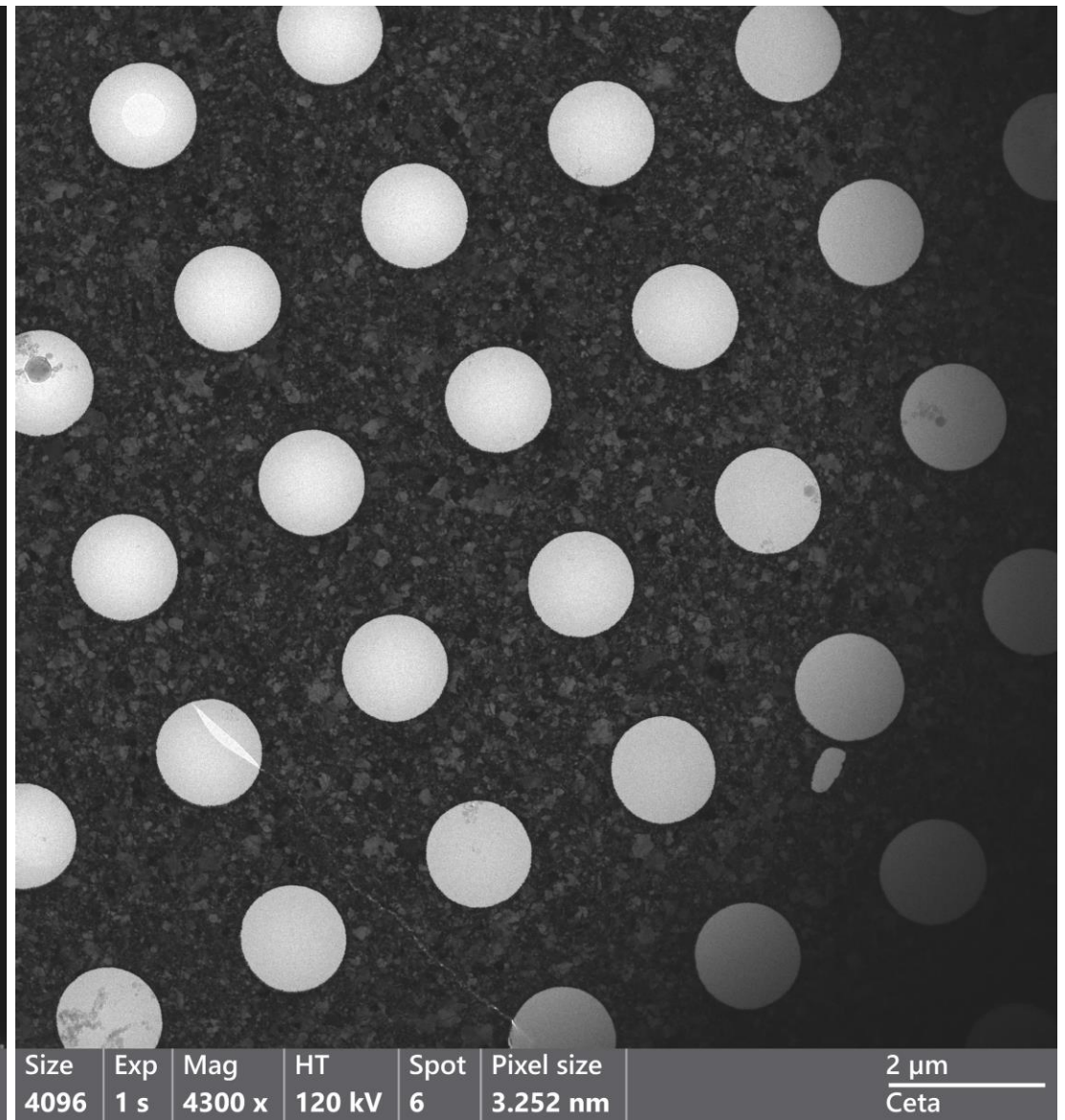
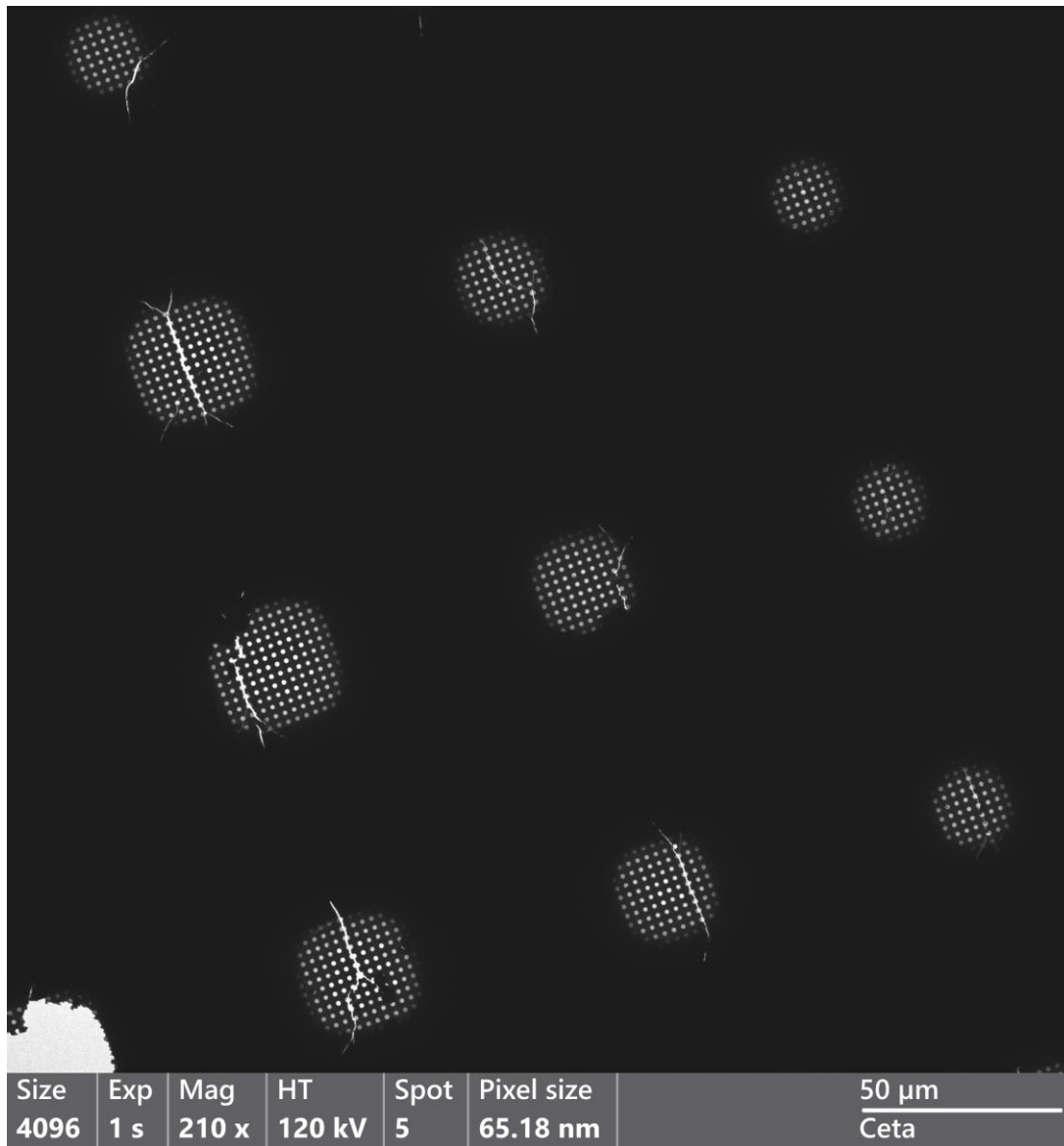


Figure 4: Grid squares from the frozen Cryo-grids. Holes from the grid squares are shown on the right. Ultra AU Foil R 1.2/1.3 grids were used.

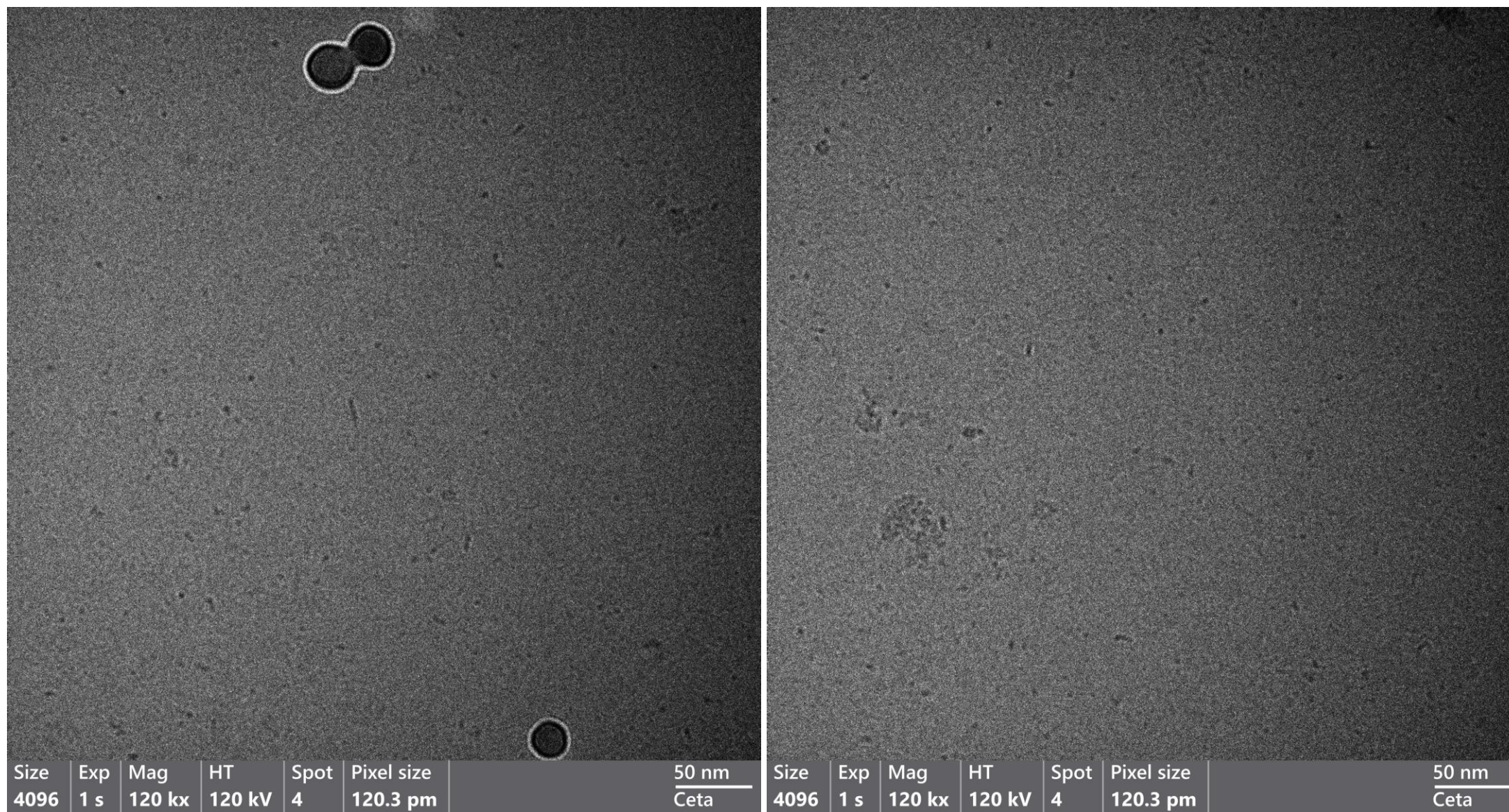


Figure 5: Cryo-micrographs from the frozen grid.

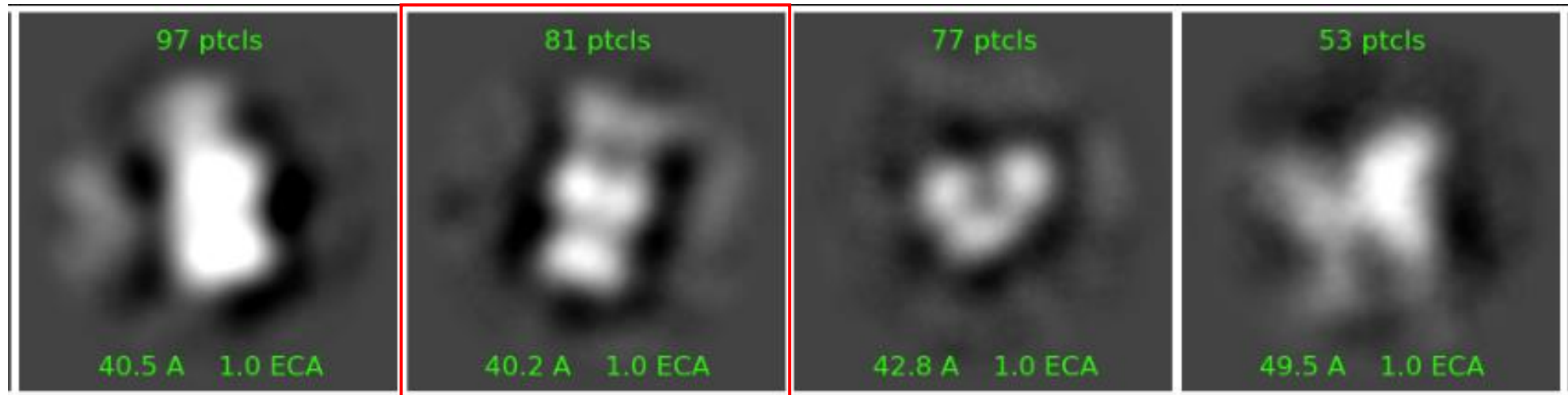


Figure 6: 2D class averages from the processing of the Cryo-micrographs. The class averages that shows the most resemblance to negative staining averages is highlighted in red.